

## Possible pitfalls in theoretical determination of ground-state crystal structures: The case of platinum nitride

Xiuwen Zhang, Giancarlo Trimarchi,\* and Alex Zunger†

National Renewable Energy Laboratory, Golden, Colorado 80401, USA

(Received 1 December 2008; published 23 March 2009)

In many theoretical studies of the properties of solids, the first and often crucial step entails the determination of the crystal structure via some form of energy minimization. Here we discuss general potential pitfalls that are often encountered in such calculations. We do so in the context of the classic zinc-blende crystal structure that underlines all octet semiconductors and was more recently invoked to explain nonoctet half-metallic magnets such as CrAs, as well as noble-metal nitrides such as PtN, PdN, and NiN. These pitfalls are related to the way in which mechanical instabilities of assumed structures are identified, discarded, and replaced. Using a more general global space-group optimization (GSGO) approach uncovers different and more complex structures that have much lower energies and do not have mechanical instabilities.

DOI: 10.1103/PhysRevB.79.092102

PACS number(s): 61.50.Ah, 81.05.Je

The fourfold-coordinated tetrahedral zinc-blende (ZB) structure of II-VI and III-V octet compounds has held the community of structural inorganic chemistry in constant fascination<sup>1,2</sup> ever since the semiconducting properties of these materials have been discovered,<sup>3</sup> making them the central architectural motifs of high technology. Indeed, the understanding of the way tetrahedral networks are stabilized by completing the electronic octet shells has long formed the basis for our understanding of the nature of the covalent bond.<sup>1,4</sup> Understandably, reports on observation of *nonoctet* binary compounds PtN,<sup>5</sup> MnAs,<sup>6</sup> and MnSe (Ref. 7) in zinc-blende or zinc-blendelike structures have never failed to attract attention, especially from the community of electronic structure theory.<sup>8–15</sup> However, the understanding of the apparent stability of nonoctet zinc-blende networks has remained elusive. For example, the prediction of a zinc-blende ground state of MnN (Ref. 15) had proven to be an artifact of the local-density approximation (LDA), disappearing after better approximation were used.<sup>14</sup> The predicted stability of numerous binary *3d* pnictides, such as CrAs, and *3d* chalcogenides, such as CrS and CrSe in the zinc-blende structure,<sup>15</sup> has mostly proven to disappear under more realistic epitaxial conditions.<sup>16</sup> Not surprisingly, the recent laser-heated diamond anvil synthesis<sup>5</sup> of PtN under high pressure and the recovery of the ensuing compound at ambient conditions, suggested by x-ray diffraction and Raman spectra to have the zinc-blende structure,<sup>5</sup> created tremendous interest<sup>8–12</sup> in this noble-metal nitride that unexpectedly is identified to be tetrahedrally bonded. The search for the crystal structure of platinum nitride has challenged and brought into focus some of the basic practices and paradigms of the theoretical attempts to determine crystal structure. Here, we address the problem of determining the crystal structure of platinum nitride via a global space-group optimization (GSGO) procedure based on an evolutionary algorithm and density-functional theory for the total-energy evaluations.<sup>17</sup> The description of our GSGO study of PtN lends itself to a discussion of four possible pitfalls of the common practices and paradigms of the theoretical attempts of crystal structure determination.

The *first* possible pitfall is that predicted lower-energy

structures (relative to a reference) are often considered to be “more stable structures” (than the reference structure). Yet, even though ZB PtN was found<sup>12</sup> in LDA calculations to be  $\sim 0.2$  eV/atom lower in energy than the rocksalt (NaCl) form, this lower-energy ZB is mechanically unstable,<sup>10</sup> failing to have a positive-definite strain energy<sup>18</sup>  $\frac{1}{2}C_{ij}e_i e_j$  (where  $C_{ij}$  are the elastic constants and  $e_i$  are the components of the strain). Similar dynamic instabilities were predicted for statically stable common structures of binary octet compounds by Ozoliņš and Zunger,<sup>19</sup> e.g., GaAs, GaP, and InP with  $\beta$ -Sn structure. Figure 1(a) demonstrates the mechanical instability of ZB PtN: the calculated energy surface of ZB PtN subjected to a deformation  $e_1=(100)$ ;  $e_2=(010)$ ;  $e_3=-(002)$ , revealing that the undistorted ZB structure is a saddle point

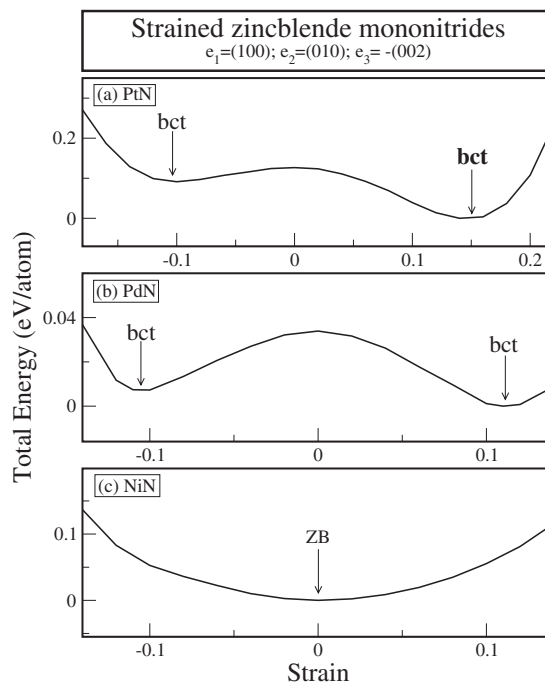


FIG. 1. Total energy vs strain curves of ZB mononitrides obtained from LDA [projector augmented wave (PAW)] calculations. We use the minimum of each curve as its energy zero point.

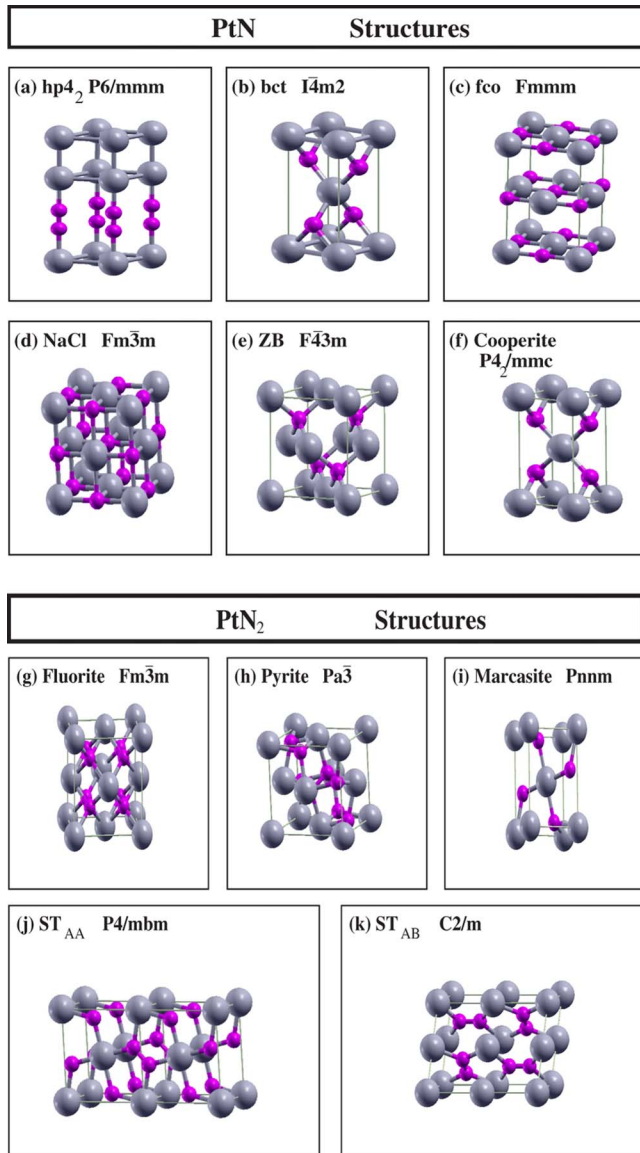


FIG. 2. (Color online) PtN and PtN<sub>2</sub> structures considered in this work. Large spheres: Pt. small spheres: N. The wurtzite (WZ) and CsCl structures can be found in Ref. 12. The bct structure shown in (b) corresponds to the lowest point in Fig. 1(a).

and that under deformation a more stable body-centered-tetragonal (bct) structure [see Fig. 2(b)] emerges. Figure 1(b) shows that ZB PdN is mechanically unstable in the same way. It is not impossible though that the ZB forms are stable at high temperatures due to the finite temperature excitations.<sup>20</sup> Figure 1(c) shows that NiN is mechanically stable in the assumed ZB structure. We will later see that this does not mean, however, that ZB NiN should exist.

The *second* possible pitfall is that the most stable structure is sometimes expected to be found by following the continuous trajectory of mechanical instability, e.g., the deformation path illustrated in Fig. 1. However, it is possible that a differently connected structure not attainable by following a continuous trajectory is yet lower in energy. Indeed, various postulated structure types that are not connected with ZB/bct have been tested.<sup>11,12</sup> We report in Fig. 3(a) the total

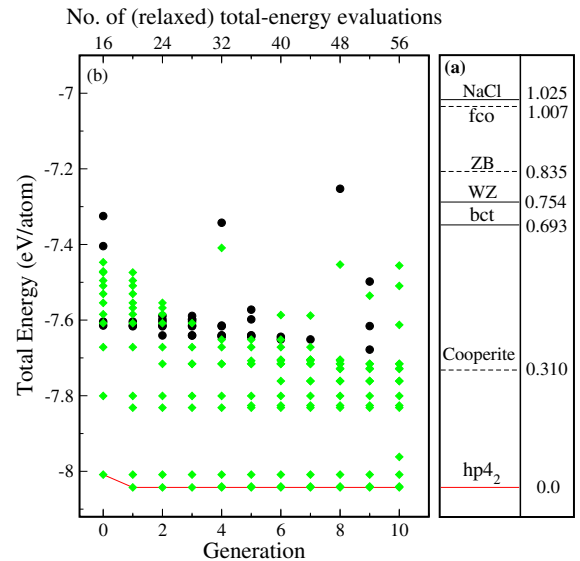


FIG. 3. (Color online) (a) Total energies (in eV/atom) of some guessed structures of PtN. See Figs. 2(a)–2(f) for the structure types. (b) Plot of the GSGO history with  $N_{pop}=16$  and  $N_{rep}=4$  performed on the Pt<sub>4</sub>N<sub>4</sub> supercell by LDA (PAW) calculations. The total energy of  $hp4_2$  PtN is  $-8.042$  eV/atom. The diamonds are the structures having N–N bonds with length smaller than 1.35 Å, and the circles are the others in the GSGO history.

energies of some guessed structures depicted in Fig. 2(a)–2(f), where the solid (dashed) line means that the structure is mechanically stable (unstable). The Cooperite structure [shown in Fig. 2(f)] has lower energy than bct. We also found that the face-centered-orthorhombic (fco) structure [see Fig. 2(c)] suggested for PtN (Ref. 11) has higher energy than ZB PtN. But there is no good way to guess which structure type to try. Indeed, the general approach of “rounding-up the usual suspects” illustrated in Fig. 3(a) can easily miss lower-energy structures.

To this end we have applied the GSGO approach, starting from random lattice vectors and random atomic positions. The GSGO method (see Refs. 21 and 22 by Trimarchi and Zunger and earlier work of Deaven and Ho,<sup>23</sup> Abrahams and Probert,<sup>24</sup> and Oganov and Glass<sup>25</sup>) uses a sequence of *ab initio* evolutions of the total energy of locally relaxed trial structures so as to seek the optimal lattice vectors and lattice decoration via a genetic-algorithm selection. A population of  $N_{pop}$  candidate structures is evolved through a sequence of generations. The structures of the initial population are randomly generated. At each new generation, the  $N_{rep}$  highest total-energy structures out of  $N_{pop}$  are replaced by new ones which are produced from the structures of the current population by performing the operations of mating and mutation. Figure 3(b) shows the plot of the GSGO history performed on a supercell Pt<sub>4</sub>N<sub>4</sub>; here we used  $N_{pop}=16$  with  $N_{rep}=4$ . We see that the lowest-energy structure found by GSGO (the  $hp4_2$  structure) has a much lower energy than the previously guessed lowest-energy Cooperite structure. The GSGO search finds the lowest-energy structure in two generations by performing about 20 *ab initio* structural relaxations. We performed GSGO on a supercell Pt<sub>4</sub>N<sub>4</sub> but found again the  $hp4_2$  structure with two Pt and two N atoms in its primitive

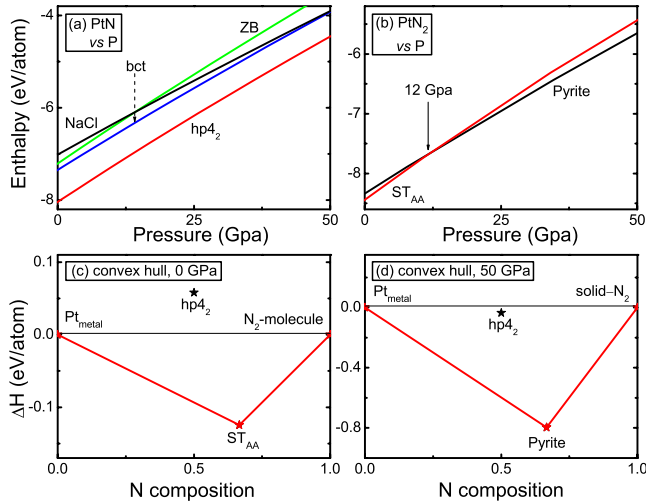


FIG. 4. (Color online) [(a) and (b)] The enthalpy ( $E+PV$ ) vs pressure curves for (a) PtN and (b) PtN<sub>2</sub>. [(c) and (d)] The convex hulls [thick line with breaking point] of Pt-N system at (c) 0 GPa and (d) 50 GPa.

cell, so the supercell size used is sufficient. The lowest-energy structure as shown in Fig. 2(a) has a hexagonal lattice with space group  $P6/mmm$  (No. 191), lattice constants  $a = 2.78 \text{ \AA}$  and  $c = 7.58 \text{ \AA}$ , and Wyckoff positions: Pt  $2e(0,0,z_{Pt})$ ,  $z_{Pt1}=0.0$ ,  $z_{Pt2}=0.67$ , N  $2e(0,0,z_N)$ ,  $z_{N1}=0.26$ ,  $z_{N2}=0.41$ . Its Pearson type is analogous to the Li<sub>3</sub>N  $hp4$  prototype, the difference being that the latter has  $1b$ ,  $2c$ , and  $1a$  Wyckoff positions. Thus we label this structure as  $hp4_2$ . The  $hp4_2$  structure is quite different from the ZB structure and cannot be found by following the mechanical instability of ZB. Unlike all other structures proposed for PtN (Fig. 2), this structure has N–N bonds. Their length is  $1.13 \text{ \AA}$ , compared with the LDA calculated bond length  $1.10 \text{ \AA}$  for the gas-phase N<sub>2</sub> molecule. Examining the structures that emerge in the GSGO history [Fig. 3(b)], we find that most of them [shown as diamonds] have N–N bonds with length smaller than  $1.35 \text{ \AA}$ .

A possible pitfall of the evolutionary-algorithm-based GSGO is that due to its stochastic nature the search for the lowest-energy structure must proceed through a series of restarts of the evolutionary sequence, and it is not guaranteed that independent sequences give the same lowest-energy structure. However, one ultimately uses the sequence that gives the lowest-energy structure. We have always found  $hp4_2$  to be the lowest-energy structure for PtN. Naturally, the accuracy and physicality of the low-energy structures uncovered by GSGO (e.g., length and binding energy of N–N bonds) are limited by the underlying energy functional used (e.g., the LDA density functional which often leads to molecular overbinding and lacks proper dispersion forces).

This  $hp4_2$  structure is mechanically stable. It has five independent elastic constants, which are calculated to be (in GPa)  $C_{11}=262$ ,  $C_{33}=915$ ,  $C_{12}=89$ ,  $C_{13}=43$ , and  $C_{44}=21$ . The mechanical stability criteria for hexagonal structures,<sup>13</sup> i.e.,  $C_{11} > |C_{12}|$ ,  $(C_{11}+C_{12})C_{33} > 2C_{13}^2$ , and  $C_{44} > 0$ , are satisfied. Furthermore, as shown in Fig. 4(a), the  $hp4_2$  structure not only is the one of lowest total energy at  $P=0$  but also is

the structure of lowest enthalpy  $H=E+PV$  under pressure.

The *third* possible pitfall of crystal structure prediction scheme is that it is sometimes expected that if a structure has the overall lowest (negative) enthalpy relative to all other examined structures *at the same composition*, it will be a ground-state structure. However, it is possible that the absolute most stable structure at one composition is unstable with respect to disproportionation into two structures of neighboring compositions. Thus, one needs to calculate the convex hull of energy (or enthalpy) vs composition.

Here we calculate only an approximate convex hull band on just a few structures because it turns out this is sufficient to illustrate the point. To calculate the approximate convex hull, we first performed GSGO calculation at another composition: PtN<sub>2</sub>, finding the lowest-energy structure to be ST<sub>AA</sub> [see in Fig. 2(j)] as found by Åberg *et al.*<sup>26</sup> Furthermore, we reproduce Åberg’s<sup>26</sup> and Crowhurst’s<sup>27</sup> results for the formation enthalpies of the ST<sub>AA</sub>, ST<sub>AB</sub> [see Fig. 2(k)], pyrite [see Fig. 2(h)], marcasite [see Fig. 2(i)], and fluorite [see Fig. 2(g)] structures, listed here from low to high formation enthalpy.

The convex hull is defined as an enthalpy vs composition plot with “breaking points” at special compositions  $x_n$  such that the structure corresponding to each such point is absolutely stable with respect to disproportionation into sums of structures of neighboring compositions.<sup>28</sup> We constructed the convex hull at  $P=0$  in Fig. 4(c) using the fcc Pt<sub>metal</sub>, the  $hp4_2$  PtN, the ST<sub>AA</sub> PtN<sub>2</sub>, and the N<sub>2</sub> molecule.  $\Delta H = H(A_xB_{1-x}) - xH(A) - (1-x)H(B)$  is the change in enthalpy when the constituents form the compound. We see that  $hp4_2$  PtN is above the convex hull. It is unstable with respect to disproportionation into Pt<sub>metal</sub>+ST<sub>AA</sub> PtN<sub>2</sub>. Thus, mechanically stable compounds [e.g., ZB NiN in Fig. 1(c)] might disappear from the phase diagrams because of disproportionation. Indeed, the theoretically predicted NiN (Refs. 29 and 30) is not a ground state as the Ni–N phase diagram contains only NiN<sub>6</sub>, Ni<sub>3</sub>N, and Ni<sub>4</sub>N.<sup>31</sup>

The *fourth* possible pitfall is that the high-pressure convex hull may be different than the low-pressure one. Figure 4(b) shows that the pyrite structure [shown in Fig. 2(h)] becomes the lowest-energy structure under 12 GPa, in agreement with the result of Åberg *et al.*<sup>26</sup> (about 11.5 GPa). To construct the convex hull at  $P=50$  GPa, we do the following: we fit calculated energies of fcc Pt<sub>metal</sub>, PtN, and PtN<sub>2</sub> over a range of volumes with a second-order Birch-Murnaghan equation of state, then we use the equation of state to get their enthalpies under pressure, respectively. The enthalpy of N<sub>2</sub> under pressure is obtained approximately by calculating the solid  $\epsilon$ -N<sub>2</sub> phase (space group:  $R\bar{3}c$ ) at zero temperature and pressure and then using its experimental equation-of-state data.<sup>32</sup> Figure 4(d) shows the convex hull of the Pt–N system at 50 GPa. We find that the  $hp4_2$  PtN is above the convex hull. Actually we have checked that the enthalpy of  $hp4_2$  PtN is always higher than that of Pt<sub>metal</sub>+PtN<sub>2</sub> in the range of 0–50 GPa, and the enthalpy difference is larger at higher pressure. Thus, the  $hp4_2$  structure should not be observable experimentally at any pressure being unstable toward phase separation into solid elements Pt and PtN<sub>2</sub>. From Fig. 4(d), we see that at 50 GPa pyrite PtN<sub>2</sub> is a ground state of the Pt–N

system: this is in agreement with the experiment<sup>27</sup> which synthesized PtN<sub>2</sub> with the pyrite structure at about 50 GPa.

We find that the bulk modulus of pyrite PtN<sub>2</sub> is 348 GPa, in agreement with the experimental result 372 GPa (Refs. 5 and 27) and the previous theoretical result 347 GPa,<sup>27</sup> while the bulk modulus of ST<sub>AA</sub> PtN<sub>2</sub> is just 83 GPa. At zero pressure, the volume of pyrite PtN<sub>2</sub> 9.12 Å<sup>3</sup>/atom is much smaller than that of ST<sub>AA</sub> PtN<sub>2</sub> 10.80 Å<sup>3</sup>/atom. The bulk moduli (volume) of NaCl, bct, and *hp*4<sub>2</sub> PtN are 294 GPa (10.66 Å<sup>3</sup>/atom), 211 GPa (11.85 Å<sup>3</sup>/atom), and 172 GPa (12.65 Å<sup>3</sup>/atom), respectively. Paiva *et al.*<sup>33</sup> calculated the lattice constants and bulk moduli of all the 4*d* transition-metal nitrides (including PdN) with ZB structure, while we found that at least ZB PdN is mechanically unstable [see Fig. 1(b)]. They found that from YN to AgN, the lattice constant (volume) decreases at first and then increases. Correspondingly, in this series the bulk modulus increases at first and then decreases. Thus for similar materials, small volume is good for high bulk modulus.

In conclusion, we performed a first-principles global space-group optimization study of Pt-N. We found the lowest-energy structure of PtN at zero pressure; but this structure is unstable toward phase separation into Pt and PtN<sub>2</sub>; so it is not a ground state of the Pt-N system. At the synthesis pressure 50 GPa,<sup>5,27</sup> pyrite PtN<sub>2</sub> is on the convex hull. The high bulk modulus of pyrite PtN<sub>2</sub> 348 GPa is possibly due to its relatively small volume at zero pressure. The four possible pitfalls in crystal structure determination, i.e., ignoring the mechanical instability, simply following the mechanical instability, ignoring the convex hull, and ignoring the difference between high-pressure convex hull and low-pressure one, were discussed.

X.Z. thanks Mayeul d'Avezac for useful discussions. This work was funded by the U.S. Department of Energy, Office of Science, Basic Energy Sciences, Materials Sciences and Engineering Division under Contract No. DE-AC36-08GO28308 to NREL.

\*Present address: Department of Physics & Astronomy, Northwestern University, Evanston, Illinois 60208.

†Alex\_Zunger@nrel.gov

<sup>1</sup>L. Pauling, *The Nature of the Chemical and Bond*, 3rd ed. (Cornell University Press, Ithaca, NY, 1960).

<sup>2</sup>E. Parthé, *Crystal Chemistry of Tetrahedral Structures* (Gordon and Breach, New York, 1964).

<sup>3</sup>N. A. Goryunova, *The Chemistry of Diamond-Like Semiconductors* (MIT, Cambridge, 1963).

<sup>4</sup>G. N. Lewis, *J. Am. Chem. Soc.* **38**, 762 (1916).

<sup>5</sup>E. Gregoryanz, C. Sanloup, M. Somayazulu, J. Badro, G. Fiquet, H. Mao, and R. J. Hemley, *Nature Mater.* **3**, 294 (2004).

<sup>6</sup>T. W. Kim, H. C. Jeon, T. W. Kang, H. S. Lee, J. Y. Lee, and S. Jin, *Appl. Phys. Lett.* **88**, 021915 (2006).

<sup>7</sup>L. A. Kolodziejwski, R. L. Gunshor, N. Otsuka, B. P. Gu, Y. Hefetz, and A. V. Nurmikko, *Appl. Phys. Lett.* **48**, 1482 (1986).

<sup>8</sup>M. B. Kanoun and S. Goumri-Said, *Phys. Rev. B* **72**, 113103 (2005).

<sup>9</sup>B. R. Sahu and L. Kleinman, *Phys. Rev. B* **71**, 041101(R) (2005).

<sup>10</sup>R. Yu and X. F. Zhang, *Appl. Phys. Lett.* **86**, 121913 (2005); *Phys. Rev. B* **72**, 054103 (2005).

<sup>11</sup>S. K. R. Patil, S. V. Khare, B. R. Tuttle, J. K. Bording, and S. Kodambaka, *Phys. Rev. B* **73**, 104118 (2006).

<sup>12</sup>L. H. Yu, K. L. Yao, Z. L. Liu, and Y. S. Zhang, *Physica B* **399**, 50 (2007).

<sup>13</sup>C.-Z. Fan, S.-Y. Zeng, L.-X. Li, Z.-J. Zhan, R.-P. Liu, W.-K. Wang, P. Zhang, and Y.-G. Yao, *Phys. Rev. B* **74**, 125118 (2006).

<sup>14</sup>J. A. Chan, J. Z. Liu, H. Raebiger, S. Lany, and A. Zunger, *Phys. Rev. B* **78**, 184109 (2008).

<sup>15</sup>W.-H. Xie, Y.-Q. Xu, B.-G. Liu, and D. G. Pettifor, *Phys. Rev. Lett.* **91**, 037204 (2003).

<sup>16</sup>Y.-J. Zhao and A. Zunger, *Phys. Rev. B* **71**, 132403 (2005).

<sup>17</sup>The density-functional calculations were performed using the pseudopotential plane-wave method, with the LDA exchange correlation functional of Perdew and Zunger,<sup>34</sup> a basis set cutoff of 520 eV, and *k*-point meshes with resolutions of  $2\pi \times 0.051 \text{ \AA}^{-1}$  and  $2\pi \times 0.034 \text{ \AA}^{-1}$  for structural relaxation and static total energy calculation,<sup>35</sup> respectively, with an energy convergence of 1 meV/atom.

<sup>18</sup>L. D. Landau and E. M. Lifshitz, *Theory of Elasticity* (Pergamon, New York, 1986).

<sup>19</sup>V. Ozoliņš and A. Zunger, *Phys. Rev. Lett.* **82**, 767 (1999).

<sup>20</sup>J. Bhattacharya and A. Van der Ven, *Acta Mater.* **56**, 4226 (2008).

<sup>21</sup>G. Trimarchi and A. Zunger, *Phys. Rev. B* **75**, 104113 (2007).

<sup>22</sup>G. Trimarchi and A. Zunger, *J. Phys.: Condens. Matter* **20**, 295212 (2008).

<sup>23</sup>D. M. Deaven and K. M. Ho, *Phys. Rev. Lett.* **75**, 288 (1995).

<sup>24</sup>N. L. Abraham and M. I. J. Probert, *Phys. Rev. B* **73**, 224104 (2006).

<sup>25</sup>A. R. Oganov and C. W. Glass, *J. Chem. Phys.* **124**, 244704 (2006).

<sup>26</sup>D. Åberg, B. Sadigh, J. Crowhurst, and A. F. Goncharov, *Phys. Rev. Lett.* **100**, 095501 (2008).

<sup>27</sup>J. C. Crowhurst, A. F. Goncharov, B. Sadigh, C. L. Evans, P. G. Morrall, J. L. Ferreira, and A. J. Nelson, *Science* **311**, 1275 (2006).

<sup>28</sup>J. Z. Liu and A. Zunger, *Phys. Rev. B* **77**, 205201 (2008).

<sup>29</sup>H.-B. Wang and D.-S. Xue, *Chin. Phys. Lett.* **21**, 1612 (2004).

<sup>30</sup>C. Paduani, *Solid State Commun.* **148**, 297 (2008).

<sup>31</sup>H. A. Wriedt, *Bull. Alloy Phase Diagrams* **6**, 558 (1985).

<sup>32</sup>H. Olijnyk, *J. Chem. Phys.* **93**, 8968 (1990).

<sup>33</sup>R. de Paiva, R. A. Nogueira, and J. L. A. Alves, *Phys. Rev. B* **75**, 085105 (2007).

<sup>34</sup>J. P. Perdew and A. Zunger, *Phys. Rev. B* **23**, 5048 (1981).

<sup>35</sup>G. Kresse and J. Furthmüller, *Comput. Mater. Sci.* **6**, 15 (1996).